

Study of Flow and Heat Transfer of $CuO - Ag / C_2H_6O_2$ Hybrid Nanofluid over a Stretching Surface with Porous Media and MHD Effect

Praveen Kumar Dadheech¹, Priyanka Agrawal¹, Sunil Dutt Purohit^{2,*}, Devendra Kumar¹

¹*Department of Mathematics, University of Rajasthan, Jaipur 302004, India*

²*Department of HEAS (Mathematics), Rajasthan Technical University, Kota 324010, India*

Received 17 August 2021; Received in revised form 26 November 2021

Accepted 04 December 2021; Available online 30 December 2021

ABSTRACT

The aim of this investigation is to study hybrid nanofluid flow past a permeable stretching sheet in is presented. With heat source/sink and uniform magnetic field the flow is investigated in porous medium. A suspension of Copper Oxide-Silver ($CuO - Ag$) nanoparticles in an ethanol glycol ($C_2H_6O_2$) based fluid with Marangoni convection is considered. The mathematical model of the flow is encountered by Runge-Kutta fourth order method using appropriate similarity transformations. As a key result, it is observed that the capacity of heat transportation of modified nanofluid is improved in comparison with nanofluids and hybrid nanofluids. Numerical solutions with graphical representation are presented. Heat transfer rate decreases when the Prandtl number and wall mass transfer parameter rise, whereas the Heat source/sink parameter has the opposite effect.

Keywords: Hybrid Nanofluid; Marangoni Convection; MHD; Porous media; Stretching Surface.

1. Introduction

A fluid called as base fluid with suspended nano-sized particles of various size and shapes is defined as nanofluid. These particles can be metallic or non-

metallic. For heat transfer applications commonly used base fluids are water, Ethylene glycol, Mineral oil, kerosene, Engine, and are generally employed in the production of nanofluids. Initially Choi [1]

investigated that by adding some nano-sized particles in any base fluid thermal conductivity can be improved. Use of these nanofluids can be seen in the industrial processes where transportation of heat is prominent as generator cooling, biomedical, nuclear safety, transformer cooling, solar heating, lubrications, welding, alcohol control, protection, MHD pumps, refrigeration and space technology. Various investigations have been presented by the researchers that how nanofluids affect the heat transfer phenomena by its size, shape, and concentration, with various base fluids and different geometries [2-8].

In continuation to this concept researchers got the idea to prepare mixture of two different nanoparticles dispersed in the basic fluids. These fluids are considered as hybrid nanofluids. With appropriate blend or combination of nanometer-sized particles dispersed into the basic fluids, improved heat transfer capacity can be obtained since advantage and disadvantage of nanoparticles can be managed in hybrid nanofluids. A number of studies have been presented by researchers proving this concept for the nanofluids using different sizes, shapes, and concentrations of nanoparticles with different base liquids, on different geometries [9-13].

Marangoni convection is the convection described with the surface tension differences at interface. These interface dissipative flows may be useful when various surface tensions exist at interface. This variation can be generated by altering the temperature or the concentration of fluid. Marangoni convective boundary layer flows of nano-liquids has their applications in various fields like thin-films, soap-films, crystals melting, vapor bubbles, welding, semiconductors, microgravity condition, material science, silicon wafers, etc. Napolitano [14] was the first who gave this phenomenon and named it. Christopher and Wang [15] studied the Prandtl numbers effects for Marangoni convective flow past

a horizontal surface. Furthermore Agrawal et al. [16] investigated radiative Marangoni convection flow of three different hybrid nanoliquids with porosity and MHD effects. Afterward this phenomenon is studied along various parameters, nanofluids and geometries by several scientists [17, 21].

Whereas various researchers have investigated nanofluids with various nanoparticles suspended in various base fluids, nonetheless, in this research $CuO - Ag / C_2H_6O_2$ nanofluids flow through a stretching surface with Marangoni convection under the effect of MHD is explored. A numerical analysis for this nanofluid presented by the graphs and discussed. A comparative study with previous findings of researchers is discussed. An excellent concurrence is achieved with the presentation of previous conclusions.

2. Mathematical formulation

The viscous in compressible nanofluids MHD Marangoni convective boundary layer flow with Heat source/sink, along permeable stretched su.

The viscous in compressible nanofluids MHD Marangoni convective boundary layer flow with Heat source/sink, along permeable stretched surface is studied in 2-D. $CuO - Ag / C_2H_6O_2$ nanofluid embedded in porous medium is considered.

It is acknowledged that the fundamental fluids and the nano-size particles are in thermal equilibrium state. The laminar fluid flow takes place at $y \geq 0$ where x-axis is considered along the surface and y-axis is considered normal to the stretching sheet. Ambient temperature T_∞ and the surface temperature T_w are assumed different. Likewise, Marangoni convection is considered, a linear relation of surface tension with temperature is given by [16]:

$$\tau = \tau_0 [1 - \bar{\tau} (T - T_\infty)] \quad (2.1)$$

Here, τ_0 is surface tension and $\bar{\tau}$ is rate of change of surface tension along Temperature. Taking these assumptions, the equation of the governing convective flows of the nanofluid is described as following [16].

$$\frac{\partial u}{\partial x} + \frac{\partial v}{\partial y} = 0, \tag{2.2}$$

$$u \frac{\partial u}{\partial x} + v \frac{\partial v}{\partial y} = \frac{\mu_{hnf}}{\rho_{hnf}} \frac{\partial^2 u}{\partial y^2} - \frac{\sigma_{hnf} B_0^2 u}{\rho_{hnf}} - \frac{\mu_{hnf}}{\rho_{hnf}} \frac{u}{k}, \tag{2.3}$$

$$u \frac{\partial T}{\partial x} + v \frac{\partial T}{\partial y} = \frac{\kappa_{hnf}}{(\rho C_p)_{hnf}} \frac{\partial^2 T}{\partial y^2} + \frac{Q_0}{(\rho C_p)_{hnf}} (T - T_\infty). \tag{2.4}$$

With boundary condition:

$$T = T_\infty + bx^2, v = v_w, \mu_{nf} \left(\frac{\partial u}{\partial y} \right) = \frac{\partial \tau}{\partial T} \frac{\partial T}{\partial x}$$

at $y = 0$ and

$$u \rightarrow 0, T \rightarrow T_\infty \text{ as } y \rightarrow \infty. \tag{2.5}$$

Here velocity components along x and y axis are u and v respectively, also C_s represents the surface heat capacity. μ_{mnf} is viscosity modified nanofluid, ρ_{mnf} is density, κ_{mnf} is thermal conductivity, σ_{mnf} is electrical conductivity and $(\rho C_p)_{mnf}$ is heat capacity. Here subscript mnf, hnf, nf and f, defined for modified nanofluids, hybrid nanofluids, nanofluids and base fluid respectively. B_0 is magnetic field strength. Also the volume fraction is ϕ also $m = 3$ is chosen for spherical type nanoparticles. Thermo-physical value of nanoliquids and base fluid are reported in Table 2.

For the hybrid nanofluids the thermo physical quantities are given by as follows [16]:

The heat capacitance is given by:

$$(\rho C_p)_{hnf} = \left\{ (1 - \phi_2) \left[(1 - \phi_1) (\rho C_p)_f + (\rho C_p)_{s1} \phi_1 \right] + (\rho C_p)_{s2} \phi_2 \right\} \tag{2.6}$$

The thermal conductivity is given as:

$$\kappa_{hnf} = \left\{ \frac{\kappa_{s2} + (n-1) \kappa_{nf} - (n-1) (\kappa_{nf} - \kappa_{s2}) \phi_2}{\kappa_{s2} + (n-1) \kappa_{nf} + (\kappa_{nf} - \kappa_{s2}) \phi_2} \right\} \kappa_{nf} \tag{2.7}$$

where

$$\kappa_{nf} = \left\{ \frac{\kappa_{s1} + (n-1) \kappa_f - (n-1) (\kappa_f - \kappa_s) \phi_1}{\kappa_{s1} + (n-1) \kappa_f + (\kappa_f - \kappa_{s1}) \phi_1} \right\} \kappa_f.$$

The effective density of hybrid nanofluid is given as follows:

$$\rho_{hnf} = \left\{ [(1 - \phi_1) \rho_f + \phi_1 \rho_{s1}] (1 - \phi_2) \right\} + \phi_2 \rho_{s2} \tag{2.8}$$

The electrical conductivity is given by:

$$\sigma_{hnf} = \left\{ \frac{2\sigma_{nf} + \sigma_{s2} - 2(\sigma_{nf} - \sigma_{s2}) \phi_2}{2\sigma_{nf} + \sigma_{s2} + (\sigma_{nf} - \sigma_{s2}) \phi_2} \right\} \sigma_{nf} \tag{2.9}$$

$$\text{where } \sigma_{nf} = \left\{ \frac{\sigma_{s1} + 2\sigma_f - 2\phi_1 (\sigma_f - \sigma_{s1})}{\sigma_{s1} + 2\sigma_f + \phi_1 (\sigma_f - \sigma_{s1})} \right\} \sigma_f.$$

Also the effective dynamic viscosity is given by:

$$\mu_{hnf} = \frac{\mu_f}{(1 - \phi_1)^{2.5} (1 - \phi_2)^{2.5}}. \tag{2.10}$$

3. Similarity Solutions

For the solution the model, the similarity transformation given below is used [13]:

$$\eta = \psi_1 y, \xi = \psi_2 x f(\eta), \theta = \frac{T - T_\infty}{T_w - T_\infty}. \tag{3.1}$$

Where

$$u = \frac{\partial \xi}{\partial y}, \quad v = -\frac{\partial \xi}{\partial x},$$

$$\psi_1 = \left(\frac{\gamma_0 \bar{\gamma} b \rho_f}{\mu_f^2} \right)^{1/3}, \psi_2 = \left(\frac{\gamma_0 \bar{\gamma} b \mu_f}{\rho_f^2} \right)^{1/3}.$$

Partial differential Eq. (2.3) and Eq. (2.4) which are non linear in nature are converted into the following equations.

$$Af''' + B(ff'' - f'^2) - \frac{\sigma_{hmf}}{\sigma_f} Mf' - K_1 Af' = 0. \tag{3.2}$$

$$\frac{C}{Pr} \frac{\kappa_{hmf}}{\kappa_f} \theta'' + \delta C\theta + f\theta' - 2f'\theta = 0. \tag{3.3}$$

Here $A = \frac{1}{(1-\phi_1)^{2.5} (1-\phi_2)^{2.5}}$,

$$B = \left\{ (1-\phi_2) \left[(1-\phi_1) + \phi_1 \frac{\rho_{s1}}{\rho_f} \right] \right\} + \phi_2 \frac{\rho_{s2}}{\rho_f}$$

and

$$C = \left\{ (1-\phi_2) \left[(1-\phi_1) + \phi_1 \frac{(\rho C_p)_{s1}}{(\rho C_p)_f} \right] \right\} + \phi_2 \frac{(\rho C_p)_{s2}}{(\rho C_p)_f}.$$

With modified initial conditions:

$$\begin{aligned} \theta(0) &= 1, f(0) = f_w, \theta(\infty) = 0, \\ f''(0) &= -\frac{2}{A}, f'(\infty) = 0. \end{aligned} \tag{3.4}$$

Here $K_1 = \frac{1}{\psi_1^2 K}$ is parameter of

permeability, $Pr = \frac{(\rho C_p)_f \nu_f}{\kappa_f}$ is Prandtl

number. Also the wall mass transfer parameter is f_w and $\delta = \frac{Q_0}{(\rho C_p)_f \psi_1 \psi_2}$ is

heat source/sink parameter and

$$M = \frac{B_0^2 \sigma_f}{\rho_f \psi_1 \psi_2}$$
 is magnetic parameter.

4. Numerical Solution

After applying suitable similarity solutions, the fundamental equations have converted to the ordinary differential equations along with boundary condition. To tackle this further, Runge-Kutta method of order four with the shooting procedure have been exercised to tackle these Eq. (3.2) and Eq. (3.3) together with the boundary conditions Eq.(3.4) turned in initial value problem, as shown below.

$$f = h_1, f' = h_2, f'' = h_3, \theta = h_4, \text{ and } \theta' = h_5.$$

$$h_3' = \frac{M}{A} \frac{\sigma_{hmf}}{\sigma_f} h_2 + K_1 h_2 + \frac{B}{A} (h_2^2 - h_1 h_3)$$

$$h_5' = \frac{Pr(2h_2 h_4 - h_1 h_5 - C\delta h_4)}{C \frac{\kappa_{hmf}}{\kappa_f}}$$

With initial conditions:

$$h_1(0) = f_w, h_3(0) = -\frac{2}{A}, h_4(0) = 1.$$

Here with above three initial conditions, two more are required i.e. $h_3(0)$ and $h_5(0)$ for the solutions. Prandtl number for $C_2H_6O_2$ is 204 considered. Taking the initial guess values for $h_3(0)$ and $h_5(0)$ and suitable finite value of $\eta (\rightarrow \infty)$, say η_∞ . After this we have computed $f'(\eta)$ and $\theta(\eta)$ at $\eta_\infty (\cong 10)$ along with conditions of boundary $f'(\eta_\infty) = 0$ and $\theta(\eta_\infty) = 0$ and for desired approximate result (degree of accuracy is 10^{-6}) we have adjusted the values of $f''(0)$ and $\theta'(0)$ taking step size as $\Delta \eta = 0.01$. To get exact results up to 10^{-7} accuracy iterated approach is used in this method.

5. Results and Discussion

Boundary layer flow with Heat source/sink, along permeable stretched surface is studied. The two-dimensional viscous in compressible hybrid nanofluid flow is considered. $CuO - Ag / C_2H_6O_2$ hybrid nanofluid embedded in porous medium is considered. Marangoni convective is considered in this investigation. Numerical simulation is performed with above described method and results are shown by graphs to explain the

impacts of several non-dimensional physical parameters for velocity profile and temperature profile.

In Fig. 1 the effects of magnetic field parameter M on velocity profile. A decreased velocity profile noticed for increased M . Imposed charismatic field creates a reverse force, called Lorentz force to the fluids the velocity field is reduced as a result of this.

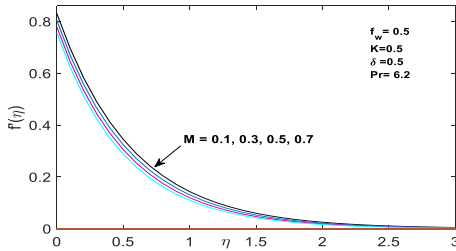


Fig. 1. Velocity profile for magnetic field parameter.

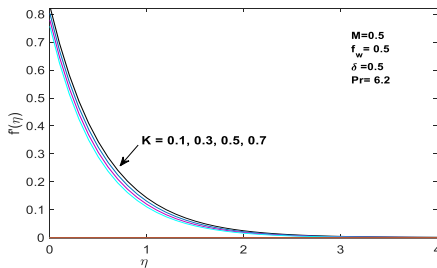


Fig. 2. Velocity profile for K.

In Fig. 2 the effects of permeability parameter K_1 on $f'(\eta)$. It is observed that with increased K_1 a decrement in $f'(\eta)$ is seen. With the fact $K \propto 1/K_1$, so with enhancement in the porosity coefficient, the permeability of the porous media decreases, resulting in a drop in fluid velocity.

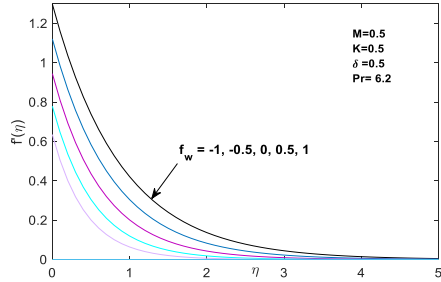


Fig. 3 Velocity profile for f_w .

In Fig. 3 and Fig. 4 the effects of f_w on $f'(\eta)$ and $\theta(\eta)$ respectively. It is observed that with increased f_w a decrement in $f'(\eta)$ (velocity profile) and $\theta(\eta)$ (temperature profile) is seen. Because the porous wall absorbs some fluids particle, the flow velocity rises, and the thermal boundary layer is lowered. As a result, the overall heat and mass transmission capacity rises.

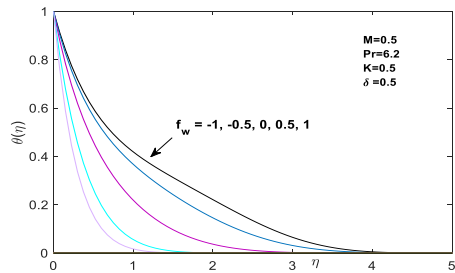


Fig. 4. Temperature profile for f_w .

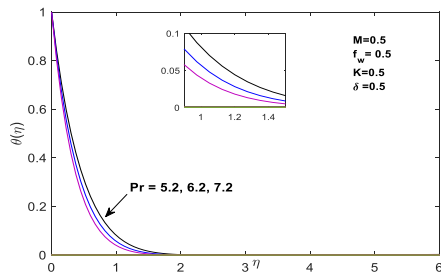


Fig. 5. Temperature profile for Pr.

In Fig. 5 the effects of Prandtl number Pr on temperature profile $\theta(\eta)$ depicted. It is observed that with

increased Pr along with $\theta(\eta)$ a decrement in temperature profile noticed. The relative effects of viscosity on thermal conductivity are referred to as Pr. This is because lower Prandtl numbers equate to better thermal conductivity, allowing heat to escape away from the heated surface faster than with bigger Prandtl numbers. In Fig. 6, the effects of heat source/sink δ on $\theta(\eta)$ are depicted. It is observed that with increase δ along with $\theta(\eta)$ an increment in temperature profile is seen.

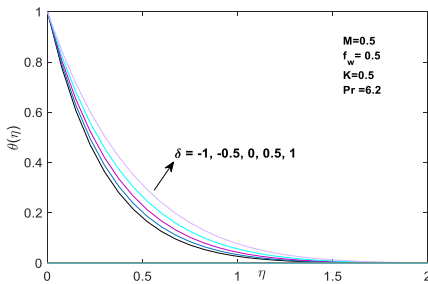


Fig. 6. Temperature profile for δ .

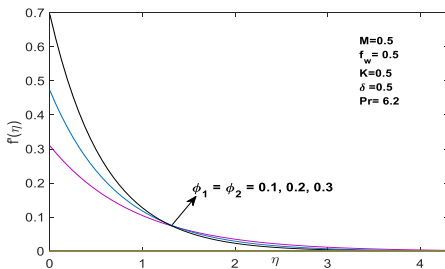


Fig. 7. Velocity profile for ϕ .

In Fig. 7 the effects of parameter volume friction $\phi_1 = \phi_2$ on $f'(\eta)$ depicted. It is observed that with increased $\phi_1 = \phi_2$ a decrement is seen in velocity curve. The fluid's velocity is lowered at the surface and raised distant from it by raising $\phi_1 = \phi_2$, which is a significant influence of $\phi_1 = \phi_2$ on the velocity profile.

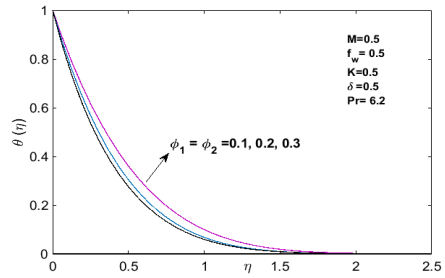


Fig. 8. Temperature profile for ϕ .

In Fig. 8 the effects of parameter volume friction $\phi_1 = \phi_2$ on $\theta(\eta)$ depicted. It is observed that with increased $\phi_1 = \phi_2$ an increment is seen in velocity curve. More nanoparticles allow additional energy to be absorbed, which might result in a higher temperature field. The calculated results are compared for Nusselt number for different values of Pr taking other parameters equals to zero is given in Table 2.

Table 2 Comparison of Nusselt number for various values of Pr taking other parameters equals to zero for $CuO - Ag / C_2H_6O_2$.

Pr	Acharya et al. [22]	Wang et al. [23]	Present study
0.7	0.453962	0.4539	0.453971
2	0.911397	0.9114	0.911393
7	1.895420	1.8954	1.895413

6. Conclusions

Heat transfer effects of a hybrid nanofluid flow are studied. MHD Marangoni convective boundary layer flow with heat source/sink, along permeable stretched surface is considered in 2-D. $CuO - Ag / C_2H_6O_2$ nanofluid embedded in porous medium is considered. In future these results can be used for other hybrid nanofluids as well as modified nanofluids. The following is a summary of the research findings:

- With increased $\phi_1 = \phi_2$ a decrement is seen in velocity field and opposite effect is seen in temperature profile.
- Decreased velocity profile is seen for increased parameters f_w , M and K .
- Heat transfer rate decreases when the Prandtl number and wall mass transfer parameter rise, whereas the Heat

source/sink parameter has the opposite effect.

Acknowledgements

The authors would like to thank anonymous referees for their useful critical comments and suggestions for improving the research paper.

Table 2. Thermo-physical properties: [17, 22].

	ρ (kg / m^3)	C_p ($J / kg K$)	k ($W / m K$)	σ (S / m)
$C_2H_6O_2$	1116.6	2382	0.249	65
CuO	6500	535.6	20	5.96×10^7
Ag	10500	235	429	3.5×10^6

References

- [1] Choi, S.U.S., Enhancing thermal conductivity of fluids with nanoparticles, The Proceedings of the 1995 ASME International Mechanical Engineering Congress and Exposition, San Francisco, ASME, FED 231/MD66, USA, (1995), pp. 99-105.
- [2] Shoaib M, Zubair G, Nisar KS, Zahoor Raja MA, Khan MI, Gowda RJP, Prasannakumara BC. Ohmic heating effects and entropy generation for nanofluidic system of Ree-Eyring fluid: Intelligent computing paradigm. International Communications in Heat and Mass Transfer 2021; 129: 105683.
- [3] Shahzad, F, Jamshed W, Ibrahim RW, Soopy Nisar K, Qureshi MA, Hussain, SM, Mohamed Isa SSP, Eid MR, Abdel-Aty A-H, Yahia IS. Comparative Numerical Study of Thermal Features Analysis between Oldroyd-B Copper and Molybdenum Disulfide Nanoparticles in Engine-Oil-Based Nanofluids Flow. Coatings 2021; 11: 1196.
- [4] Ali K, Ahmad S, Nisar KS, Faridi AA, Ashraf M. Simulation analysis of MHD hybrid Cu-Al₂O₃/H₂O nanofluid flow with heat generation through a porous media. Int J Energy Res. 2021; 1-15. <https://doi.org/10.1002/er.7016>
- [5] GuptaR, Gaur M, Dadheech PK, Agrawal P. Numerical study of radiative MHD slip flow of Williamson fluid in porous medium over a melting stretching surface. Bulletin Monumental 2021; 22(11): 52-75.
- [6] Kumar D, Sinha S, Sharma A, Agrawal P, Dadheech, PK. Numerical study of chemical reaction and heat transfer of MHD slip flow with Joule heating and Soret–Dufour effect over an exponentially stretching sheet. Heat Transfer 2021; 1-25. doi:10.1002/htj.22382
- [7] Wang X-Q, Majumdar AS. Heat transfer characteristics of nanofluids: a review. Int J Thermal Sci. 2007; 46:1-19.
- [8] Xuan YM, Roetzel W. Conceptions of heat transfer correlation of nanofluids. International Journal Communications in Heat and Mass Transfer 2020; 43: 3701-7.
- [9] Dadheech PK, Agrawal P, Mebarek-Oudina F, Abu-Hamdeh N, Sharma, A. Comparative Heat Transfer Analysis of MoS₂/C₂H₆O₂ and SiO₂-MoS₂/C₂H₆O₂ Nanofluids with Natural

- Convection and Inclined Magnetic Field. *Journal of Nanofluids* 2020; 9(3): 161-7.
- [10] Hazarika S, Ahmed S, Chamkha AJ. Analysis of Platelet Shape Al₂O₃ and TiO₂ on Heat Generative Hydromagnetic Nanofluids for the Base Fluid C₂H₆O₂ in a Vertical Channel of Porous Medium. *Walailak Journal of Science & Technology* 2021; 18 (14): 1-19.
- [11] Biswas N, Manna NK, Chamkha AJ, Mandal DK. Effect of surface waviness on MHD thermo-gravitational convection of Cu-Al₂O₃-water hybrid nanofluid in a porous oblique enclosure. *Physica Scripta* 2021; 96(10): 105002.
- [12] Agrawal P, Dadheech PK, Jat RN, Nisar KS, Bohra M, Purohit SD. Magneto Marangoni flow of γ -AL₂O₃ nanofluids with thermal radiation and heat source/sink effects over a stretching surface embedded in porous medium. *Case Studies in Thermal Engineering* 2021; 23: 100802.
- [13] Mathur P, Mishra SR, Purohit SD, Bohra M. Entropy generation in a micropolar fluid past an inclined channel with velocity slip and heat flux conditions: Variation parameter method. *Heat Transfer* 2021; 1-15.
- [14] Napolitano LG. Marangoni boundary layers, in: *Proc. 3rd European Symposium on Material Science in Space*. Grenoble, ESA SP-142, June (1979).
- [15] Christopher DM, Wang BX. Prandtl number effects for Marangoni convection over a flat surface. *Int. J. Therm. Sci.* 2001;40:564-70.
- [16] Agrawal P, Dadheech PK, Jat RN, Baleanu D, Purohit SD. Radiative MHD hybrid-nanofluids flow over a permeable stretching surface with heat source/sink embedded in porous medium. *International Journal of Numerical Methods for Heat & Fluid Flow* 2021; 31(8):2818-40.
- [17] Ganesh NV, Kameswaran PK, Al-Mdallal QM, Abdul Hakeem AK, Ganga B. Non-Linear Thermal Radiative Marangoni Boundary Layer Flow of Gamma Al₂O₃ Nanofluids Past a stretching Sheet. *Journal of Nanofluids* 2018; 7 :1-7.
- [18] Al-Mdallal QM, Indumathi N, Ganga B, Abdul Hakeem AK. Marangoni radiative effects of hybrid-nanofluids flow past a permeable surface with inclined magnetic field. *Case Studies in Thermal Engineering* 2020; 17: 100571.
- [19] Dadheech PK, Agrawal P, Sharma A, Nisar KS, Purohit SD. 2021, Marangoni convection flow of γ -Al₂O₃ nanofluids past a porous stretching surface with thermal radiation effect in the presence of an inclined magnetic field. *Heat Transfer* 2022; 51:534-50.
- [20] Dadheech PK, Agrawal P, Sharma A, Mdallal QA, Purohit SD. Entropy analysis for radiative inclined MHD slip flow with heat source in porous medium for two different fluids. *Case Studies in Thermal Engineering* 2021; 28: 101491.
- [21] Jat RN, Agrawal P, Dadheech PK. MHD boundary layer flow and heat transfer of Caisson fluid over a moving porous plate with viscous dissipation and thermal radiation effects. *Journal of Rajasthan Academy of Physical Sciences* 2017; 16 (3-4): 211-32.
- [22] Acharya N, Maity S, Kundu PK. Influence of inclined magnetic field on the flow of condensed nanomaterial over a slippery surface: the hybrid visualization. *Appl Nanosci.* 2020; 10: 633-47.
- [23] Wang CY. Free convection on a vertical stretching surface. *J Appl Math Mech (ZAMM)* 1989; 69: 418-20.